Clim. Past Discuss., 7, 2391–2411, 2011
www.clim-past-discuss.net/7/2391/2011/
doi:10.5194/cpd-7-2391-2011

Climate of the Past Discussions

The role of orbital forcing, carbon dioxide and regolith in 100 kyr glacial cycles

A. Ganopolski and R. Calov

Potsdam Institute for Climate Impact Research, Potsdam, Germany

Received: 24 June 2011 – Accepted: 28 June 2011 – Published: 18 July 2011

Correspondence to: A. Ganopolski (andrey@pik-potsdam.de)

Published by Copernicus Publications on behalf of the European Geosciences Union.

Abstract

The origin of the 100 kyr cyclicity which dominates ice volume variations and other climate records over the past million years remains debatable. Here, using a comprehensive Earth system model of intermediate complexity, we demonstrate that both strong 100 kyr periodicity in the ice volume variations and the timing of glacial terminations during past 800 kyr can be successfully simulated as the direct, strongly nonlinear response of the climate-cryosphere system to the orbital forcing alone, if the atmospheric CO_2 concentration stays below its typical interglacial value. The existence of long glacial cycles is primarily attributed to the North American ice sheet and requires presence of a large continental area with exposed rocks. We show that the sharp peak in the power spectrum of ice volume at 100 kyr period results from the long glacial cycles being synchronized with the Earth's orbital eccentricity. Although 100 kyr cyclicity can be simulated with a constant CO_2 concentration, temporal variability in the CO_2 concentration plays an important role in the amplification of the 100 kyr cycles.

1 Introduction

Although it is generally accepted that, as postulated by the Milankovitch theory (Milankovitch, 1941), Earth's orbital variations play an important role in Quaternary climate dynamics, the nature of glacial cycles still remains poorly understood. One of the major challenges to the classical Milankovitch theory is the presence of 100 kyr cycles that dominate global ice volume and climate variability over the past million years (Hays et al., 1976; Imbrie et al., 1993; Paillard, 2001). This periodicity is practically absent in the principal "Milankovitch forcing" – variations of summer insolation at high latitudes of the Northern Hemisphere (NH). The eccentricity of Earth's orbit does contain periodicities close to 100 kyr, but the direct effect of the eccentricity on Earth's global energy balance is very small. Moreover, eccentricity variations are dominated by a 400 kyr cycle which is also seen in some older geological records (e.g. Zachos et al., 1997), but is practically absent in the frequency spectrum of the ice volume variations for the last million years. In view of this long-standing problem, it was proposed that the 100 kyr cycles do not originate directly from the orbital forcing but rather represent internal oscillations in the climate-cryosphere (Gildor and Tziperman, 2000) or climate-cryosphere-carbonosphere system (e.g. Saltzman and Maasch, 1988; Paillard and Parrenin, 2004). It was also suggested that the 100 kyr cycles result from the terminations of ice sheet buildup by each second or third obliquity cycle (Huybers and Wunsch, 2005), or each fourth or fifth precessional cycle (Ridgewell et al., 1999). None of these hypotheses, however, explain the robust phase relationship between glacial cycles and 100-kyr eccentricity cycles seen in the paleoclimate records (Hays et al., 1976; Berger et al., 2005; Lisiecki, 2010).

A number of modeling studies were undertaken in recent decades to understand the origin of 100 kyr glacial cycles. Simulations with simplified climate-cryosphere models (Pollard, 1983; Deblonde and Peltier, 1991; Berger et al., 1999; Crowley and Hyde, 2008) have shown that 100 kyr cyclicity does appear in ice volume variations driven by orbital variations alone. However, in most cases, the simulated 100 kyr cycles were weaker than in the paleoclimate records and were additionally accompanied by pronounced variability at another eccentricity frequency – 400 kyr – which is not seen in the spectra of reconstructed ice volume. It was only when realistic CO_2 forcing was applied in addition to orbital forcing that realistic simulations of the glacial cycles became possible (Berger et al., 1998). The notable exception is the work by Pollard (1983) where after adding several nonlinear process, the model forced by orbital variations alone, simulates strong 100 kyr cycles in agreement with the ice volume reconstructions available at that time. It is interesting to note that the agreement is even more impressive when Pollard's modelling results are compared to the most recent reconstructions of the ice volume.

Although simplified climate-cryosphere models demonstrate the possibility of the appearance of the 100 kyr cycle as a direct response of the climate-cryosphere system to the orbital forcing, due to their simplicity (usually these models were based on a one-dimensional ice sheet model and an energy balance atmosphere model), doubt remains that these results are not fully applicable to the real world. Moreover, the presence of 400 kyr cycles in many simulations remains an obvious problem. Therefore, it is crucial to corroborate earlier results and further advance the understanding of glacial cycles by using more physically based and geographically explicit climate-cryopshere models. While coupled GCMs still remains too expensive for simulating glacial cycles, models of intermediate complexity (EMICs, Claussen et al., 2001) can be coupled to 3-D ice sheet models and are sufficiently computationally efficient to perform simulations of the glacial cycles. Using CLIMBER-2 coupled to different ice sheet models, Bonelli et al. (2009) and Ganopolski et al. (2010) performed simulations of the last glacial cycles, Calov and Ganopolski (2005) analysed the stability of the climate-cryopshere system in the phase space of Milankovitch forcing and Bauer and Ganopolski (2010) reported simulations of the last four glacial cycles. Here we will present a large suite of simulations for the last 800 kyr, a period of time which was dominated by 100 kyr cyclicity.

2 Model description and experimental setup

The model used in the study is the most recent version of the Earth system model of intermediate complexity CLIMBER-2 (Petoukhov et al., 2000; Ganopolski et al., 2001; Brovkin et al., 2002) which includes a 3-D thermomechanical ice sheet model (Greve, 1997). The ice sheet model is only applied to the Northern Hemisphere and is coupled to the climate component via a high-resolution, physically-based surface energy and mass balance interface (Calov et al., 2005), which explicitly accounts for the effect of aeolian dust deposition on snow albedo. Here we use the same approach as in Ganopolski et al. (2010) but apply it to simulate glacial cycles over the past 800 000 years.

In all experiments the equilibrium state of the climate-cryosphere system obtained for present-day conditions was used as the initial condition and the model was run from

860 kyr BP until the present. The first 60 000 years, representing the model spin-up, were not used for further analysis.

In the first Baseline Experiment (referred to hereafter as BE), we prescribed variations in orbital parameters following Berger (1978) and the equivalent CO_2 concentration, which accounts for the radiative forcing of three major greenhouse gases – carbon dioxide, methane and nitrous oxide. Their concentrations were derived from the Antarctic ice cores (Petit et al., 1999; EPICA community members, 2004). The method used to calculate the equivalent CO_2 concentration is described in Ganopolski et al. (2010). A continuous record of N_2O is not available for the last 800 kyr, but existing data suggest that, to the first approximation, the N_2O concentration has a temporal dynamic similar to CO_2. Therefore, we assumed that the radiative forcing of N_2O (relative to preindustrial) is 20 % of that for CO_2 during the whole simulated period, i.e. the ratio between radiative forcings of N_2O and CO_2 is the same as at the LGM.

Although, concentrations of GHGs from the ice cores are only available for the last 800 000 years, the time 800 kyr BP is not the best choice for the beginning of the simulations, because it was close to a glacial maximum and therefore would require initialization of the large continental ice sheets in the Northern Hemisphere. For this reason, we begin our simulations at 860 kyr BP, which corresponds to the MIS 21 interglacial, for which we can use the equilibrium present-day climate state as initial conditions. However, this choice of the initial state requires prescription of the equivalent CO_2 concentration for the time interval when reliable data for GHGs concentration are not yet available. To extend the time series of equivalent CO_2 concentration beyond 800 kyr BP, we made use of a close correlation between the total radiative forcing of GHGs and benthic $\delta^{18}O$ stack (Lisiecki and Raymo, 2005) observed for the last 800 kyr. By using a simple linear regression, we calculated equivalent CO_2 concentration for these initial 60 kyr. Since this period was considered as the model spin-up and was not used for the further analysis, the accuracy of this reconstruction of the equivalent CO_2 is not crucial for the results presented in the paper.

CPD
7, 2391–2411, 2011

In addition to the BE, we performed a large suite of experiments with constant CO_2, modified orbital forcing and terrestrial sediment mask. These experiments are summarized in Table 1.

3 Results

3.1 Baseline experiment

Figure 1 shows that the model successfully simulates the waning and waxing of the ice sheets with dominant 100 kyr periodicity and a pronounced asymmetry of the glacial cycles. For the second half of the run, modeling results agree favorably with reconstructed variations of global sea level by (Waelbroeck et al., 2002). For the earlier part of the modeled period, reliable reconstructions of the global ice volume are absent, and the benthic $\delta^{18}O_c$ stack by Lisiecki and Raymo (2005) was used for comparison. Since benthic $\delta^{18}O_c$ is not an accurate proxy for the ice volume, we computed the model's equivalent of $\delta^{18}O_c$ from simulated global ice volume and the deep ocean temperature using a simple relationship between $\delta^{18}O_c$ and the ice volume and the deep ocean temperatures (Duplessy et al., 1991). In addition, based on the results of simulations of the Antarctic Ice sheet evolution during the last glacial cycle (Huybrechts, 2002), we assume that the Southern Hemisphere contributed an additional 10 % to the global ice volume variations. Computed in this way, the modeled $\delta^{18}O_c$ agrees well with the empirical stack (Fig. 1d). The frequency spectra of modeled and empirical $\delta^{18}O_c$ are also in good agreement (Fig. 2a). All three major peaks – 100, 41 and 23 kyr are reproduced with the dominance of 100 kyr cycle and a weaker precessional cycle, even though the modeled $\delta^{18}O_c$ contains more spectral power in the precessional band than the empirical spectrum. It is also important that all simulated terminations occur at the right time. This realistic simulation performed with prescribed orbital and GHG forcings represents an important test for the model. However, such an experiment does not answer the question about the origin of the strong 100 kyr cycles, since it is possible that

CPD
7, 2391–2411, 2011

the dominant 100 kyr periodicity and the correct timing of glacial terminations are solely attributed to the prescribed GHG forcing, the temporal dynamics of which strongly resembles the ice volume.

3.2 Experiments with constant CO_2

To clarify whether the 100 kyr cycles directly originate from the orbital forcing, we performed a set of additional experiments (referred to hereafter as CC*n*, where *n* is the prescribed CO_2 concentration in ppm, also see Table 1) with the same orbital forcing as in the BE described above, but maintaining a constant CO_2 concentration in time. We performed ten experiments with the CO_2 concentration ranging from 180 to 300 ppm (for every 20 ppm). Figure 3a shows a representative subset of these simulations, while Fig. 4 shows the results of all CC*n* experiments for the range of CO_2 concentrations from 200 to 280 ppm. Quasi-regular glacial cycles are simulated for CO_2 concentrations below 300 ppm, with the magnitude of the ice volume variations increasing for decreasing CO_2. For CO_2 concentrations above 260 ppm, simulated glacial cycles are dominated by obliquity and precession, but for lower CO_2 concentrations, the model simulates long and asymmetric glacial cycles with a strong peak in the 100 kyr band in the frequency spectra (Figs. 2c and 3a). It is also noteworthy that, together with 100 kyr peak, another one, although weaker, appears in the 400 kyr band. This peak is also seen in the results of previous simulations of the glacial cycles and coincides with another eccentricity periodicity. Therefore, the presence of both 100 and 400 kyr periodicities strongly indicates a direct relationship of the long glacial cycles with eccentricity variations. Unlike Crowley and Hyde (2008), who found the existence of 100 kyr cycles in a narrow range of CO_2 concentrations, in our simulations, 100 kyr cycles are robust over a broad range of CO_2 concentrations (180–260 ppm).

It is important to note that in the simulations with a constant CO_2 concentration below 260 ppm, not only are the ice volume changes dominated by the 100 kyr cycles, but simulated glacial terminations also occur at the same time as in the experiment with prescribed time-dependent CO_2 and, within the dating accuracy, in good agreement with paleoclimate reconstructions. The only exception is for MIS11 (around 400 kyr BP), when complete deglaciation of the Northern Hemisphere does not occur in the experiments with low CO_2 concentrations. The later fact is not surprising since the orbital forcing was weak during MIS11 due to low eccentricity. Whether this problem implies that for this specific termination the role of CO_2 is more important than for the others or that the model is still not sufficiently non-linear to remove the ice under MIS11 orbital forcing cannot be answered within the context of this study.

Although 860 kyr BP represents a convenient time to start simulations of the last glacial cycles, since it corresponds to an interglacial state and therefore does not require initialisation of the continental ice sheets, it is theoretically possible, that this choice can be crucial for the timing of simulated glacial terminations and therefore a good agreement between simulated and real glacial terminations would be accidental. To show that this is not the case and the timing of the glacial terminations is solely controlled by the orbital forcing, we performed an additional set of model simulations for constant CO_2 concentration equal to 220 ppm, where we began the model runs at the different astronomical times: 800, 820, 840, ... 900 kyr BP using the same (interglacial) initial conditions. These experiments are referred as CC220/*m*, where *m* denotes the timing of the start of the experiment. Figure 5 shows that in all experiments CC220/*m* the simulated ice volume converged within one glacial cycle to the same solution. Therefore, the temporal dynamics and timings of glacial terminations after the model spin-up are not sensitive to the choice of the beginning of the models runs.

3.3 Sensitivity of glacial cycles to different components of the orbital forcing

To find which component of the orbital forcing is responsible for the existence of 100 kyr cyclicity, we performed a suite of additional experiments in which, similar to the CC*n* set, the CO_2 concentration was held constant but the orbital forcing was modified. In the first set of experiments (referred as COB*n*), we removed the effect of obliquity variations by setting obliquity constant in time and equal to its average value over the simulated period (Fig. 6b). As shown in Fig. 3b, the removal of obliquity variations does not qualitatively affect the simulated glacial cycles. For sufficiently low CO_2 concentrations, long glacial cycles with a sharp maximum in the frequency spectra at 100 kyr periodicity are simulated (Fig. 2d). However, fixing of the obliquity results in a narrower range of CO_2 concentrations for which 100 kyr cyclicity dominates the frequency spectra. In addition, fixing obliquity makes glacial terminations less robust for the periods of low eccentricity, in particular, during the most recent termination. At the same time, all terminations that occurred during high eccentricity are correctly simulated in the COB*n* experiments.

In the complimentary set of experiments (referred as CECn/e), we modified the orbital forcing by setting eccentricity constant in time, with a value in the range 0–0.05, which covers real variations of eccentricity (Fig. 6c). Variations of obliquity and precession were the same as in reality. For eccentricity lower than 0.02, the model failed to simulate pronounced glacial cycles and for eccentricity of 0.04 and higher, the ice volume variations are dominated by precession (not shown). However, for intermediate values of eccentricity (0.02 and 0.03) and sufficiently low CO_2 concentrations, the model simulates long glacial cycles (Fig. 3c). Moreover, many (but not all) simulated glacial terminations occur in the CEC220/0.02 experiments at the right time. However, the frequency spectra of ice volume variations in CECn/e experiments lack a sharp peak in the 100 kyr band (Fig. 2e). In fact, the shape of the frequency spectrum in these experiments is very sensitive to the CO_2 level and the maximum of spectral power tends to occur at one or multiples of obliquity periods, rather than at 100 kyr. Therefore, in our experiments, obliquity variations themselves are not responsible for the existence of the 100 kyr cycles, but they do contribute to the robustness of the long glacial cycles.

3.4 The role of regolith

To gain insight into the possible origin of the mid-Pleistocene transition (around 1 million years ago), when the dominant periodicity of the glacial cycles changed from 40 kyr

CPD
7, 2391–2411, 2011

to 100 kyr (Ruddiman et al., 1989), we performed a set of model experiments identical to the CC*n* set, except for the spatial distribution of terrestrial sediments. Namely, we prescribed the presence of thick terrestrial sediment layer for all continental grid cells, while in the previous, we use a realistic distribution of terrestrial sediments. This set of experiments is referred as REG*n*. With the continents completely covered by sediments, 100 kyr cyclicity is absent in the simulated ice volume for the whole range of prescribed CO_2 concentrations and the ice volume variations are of a smaller magnitude than in the CC*n* experiments. This result lends support to the hypothesis that the gradual removal of the sediments from the large area of North America stabilized the North American ice sheet and led to the regime change in glacial cycles (Clark and Pollard, 1998). It is important to note that the presence of terrestrial sediments in our model has a dual effect on the ice sheets: (i) it enhances the velocity of the ice sheet sliding in the areas where the ice base is at the pressure melting point and (ii) it increases production of glaciogenic dust around the margins of the ice sheets, which affects surface albedo and facilitates surface melt (Ganopolski et al., 2010). Both factors affect the stability of the ice sheets by making them more sensitive to changes in orbital forcing. Only when a large area of North America is free of sediments can the ice sheet survive several precessional cycles, before it expands well into the area covered by the sediments, making the ice sheet more sensitive to summer insolation changes.

4 Conclusions

Results of our experiments support the notion that 100 kyr cycles represent a direct, strongly nonlinear response of the climate-cryosphere system to orbital forcing and it is directly related to the corresponding eccentricity period. In terms of nonlinear dynamics, this link can be interpreted as the phase-locking of the long glacial cycles to the shortest (100 kyr) eccentricity cycles. Physically, this phase-locking is explained by the fact that the ice sheets tend to grow monotonously during periods of low eccentricity

CPD
7, 2391–2411, 2011

A. Ganopolski and R. Calov

and reach their critical size (volume) around the minimum of eccentricity. When eccentricity starts to grow, the first sufficiently large positive anomaly in orbital forcing can lead to the rapid and irreversible meltback of the Northern Hemisphere ice sheets. This mechanism requires the existence of long glacial cycles which, in turn, require sufficiently low CO_2 concentrations and the presence of a large area of the continents free of sediment. The CO_2 concentration not only determines the dominant regime of glacial variability, but also strongly amplifies 100 kyr cycles. Therefore, realistic simulations of the glacial cycles require comprehensive Earth system models that include both physical and bio-geochemical components of the Earth system.

Acknowledgements. We would like to thank Ralf Greve for providing us with the ice sheet model SICOPOLIS and Alexander Robinson for useful suggestions. This project was partly funded by the Deutsche Forschungsgemeinschaft CL 178/4-1 and CL 178/4-2.

References

Bauer, E. and Ganopolski, A.: Aeolian dust modeling over the past four glacial cycles with CLIMBER-2, Global Planet. Change, 74, 49–60, 2010.

Berger, A.: Long-term variations of daily insolation and Quaternary climatic change, J. Atmos. Sci., 35, 2362–2367, 1978.

Berger, A., Loutre, M. F., and Gallee, H.: Sensitivity of the LLN climate model to the astronomical and CO_2 forcings over the last 200 ky, Clim. Dynam., 14, 615–629, 1998.

Berger, A., Li, X. S., and Loutre, M. F.: Modeling northern hemisphere ice volume over the last 3 million years, Quat. Sci. Rev., 18, 1–11, 1999.

Berger, A., Melice, J. L., and Loutre, M. F.: On the origin of the 100-kyr cycles in the astronomical forcing, Paleoceanography, 20, PA4019, doi:10.1029/2005PA001173, 2005.

Bonelli, S., Charbit, S., Kageyama, M., Woillez, M.-N., Ramstein, G., Dumas, C., and Quiquet, A.: Investigating the evolution of major Northern Hemisphere ice sheets during the last glacial-interglacial cycle, Clim. Past, 5, 329–345, doi:10.5194/cp-5-329-2009, 2009.

Brovkin, V., Bendtsen, J., Claussen, M., Ganopolski, A., Kubatzki, C., Petoukhov, V., and Andreev, A.: Carbon cycle, vegetation and climate dynamics in the Holocene: experiments with

the CLIMBER-2 model, Global Biogeochem. Cycles, 16, 1139, doi:10.1029/2001GB001662, 2002.
Calov, R. and Ganopolski, A.: Multistability and hysteresis in the climate-cryosphere system under orbital forcing, Geophys. Res. Lett., 32, L21717, doi:10.1029/2005GL024518, 2005.
Calov, R., Ganopolski, A., Claussen, M., Petoukhov, V., and Greve, R.: Transient simulation of the last glacial inception. Part I: Glacial inception as a bifurcation of the climate system, Clim. Dynam., 24, 545–561, doi:10.1007/s00382-005-0007-6, 2005.
Clark, P. U. and Pollard, D.: Origin of the Middle Pleistocene Transition by ice sheet erosion of regolith, Paleoceanography, 13, 1–9, 1998.
Claussen, M., Mysak, L. A., Weaver, A. J., Crucifix, M., Fichefet, T., Loutre, M. F., Weber, S. L., Alcamo, J., Alexeev, V. A., Berger, A., Calov, R., Ganopolski, A., Goosse, H., Lohman, G., Lunkeit, F., Mokhov, I. I., Petoukhov, V., Stone, P., and Wang, Z.: Earth system models of intermediate complexity: closing the gap in the spectrum of climate system models, Clim. Dyn., 18, 579–586, 2002
Crowley, T. J. and Hyde, W. T.: Transient nature of late Pleistocene climate variability, Nature, 456, 226–230, 2008.
Deblonde, G. and Peltier, W. R.: Simulations of continental ice sheet growth over the last glacial-interglacial cycle: Experiments with a one-level seasonal energy balance model including realistic geography, J. Geophys. Res., 96, 9189–9215, 1991.
Duplessy, J.-C., Labeyrie, L., Juillet-Leclerc, A., Maitre, F., Duprat, J., and Sarnthein, M.: Surface salinity reconstruction of the North Atlantic Ocean during the last glacial maximum, Oceanoogica Acta, 14, 311–324, 1991.
EPICA community members: Eight glacial cycles from an Antarctic ice core, Nature, 429, 623–628, 2004.
Ganopolski, A., Petoukhov, V., Rahmstorf, S., Brovkin, V., Claussen, M., Eliseev, A., and Kubatzki, C.: CLIMBER-2: a climate system model of intermediate complexity. Part II: Model sensitivity, Clim. Dynam., 17, 735–751, 2001.
Ganopolski, A., Calov, R., and Claussen, M.: Simulation of the last glacial cycle with a coupled climate ice-sheet model of intermediate complexity, Clim. Past, 6, 229–244, doi:10.5194/cp-6-229-2010, 2010.
Gildor, H. and Tziperman, E.: A sea ice climate switch mechanism for the 100-kyr glacial cycles, J. Geophys. Res., 106(C5), 9117–9133, 2001.
Greve, R.: A continuum-mechanical formulation for shallow polythermal ice sheets, Philos.

Trans. R. Soc. Lond. A, 355, 921–974, 1997.
Hays, J. D., Imbrie, J., Shackleton, N. J.: Variations in the earth's orbit: pacemaker of the Ice Ages, Science, 194, 1121–1132, 1976.
Huybers, P. and Wunsch, C.: Obliquity pacing of the late Pleistocene glacial terminations, Nature, 434, 491–494, 2005.
Huybrechts, P.: Sea-level changes at the LGM from ice-dynamics reconstructions of the Greenland and Antarctic ice sheets during the glacial cycles, Quat. Sci. Rev., 21, 203–231, 2002.
Imbrie, J., Berger, A., Boyle, E. A., Clemens, S. C., Duffy, A., Howard, W. R., Kukla, G., Kutzbach, J., Martinson, D. G., McIntyre, A., Mix, A. C., Molfino, B., Morley, J. J., Peterson, L. C., Pisias, N. G., Prell, W. L., Raymo, M. E., Shackleton, N. J., and Toggwiler, J. R.: On the structure and origin of major glaciation cycles, 2. The 100,000-year cycle, Paleoceanography, 8, 699–735, 1993.
Lisiecki, L. E.: Links between eccentricity forcing and the 100,000-year glacial cycle, Nature Geosci., 3, 349–352, 2010.
Lisiecki, L. E. and Raymo, M. E.: A Pliocene-Pleistocene stack of 57 globally distributed benthic δ^{18}O records, Paleoceanography, 20, PA1003, doi:10.1029/2004PA001071, 2005.
Milankovitch, M.: Kanon der Erdbestrahlung und Seine Andwendung auf das Eiszeitenproblem, Royal Serbian Academy Special Publication 132, Belgrade, Serbia, 1941.
Paillard, D.: Glacial cycles: Toward a new paradigm, Rev. Geophys., 39, 325–346, 2001.
Paillard, D. and Parrenin, F.: The Antarctic ice sheet and the triggering of deglaciations, EPSL, 227, 263–271, 2004.
Petit, J. R., Jouzel, J., Raynaud, D., Barkov, N. I., Barnola, J. M., Basile, I., Bender, M., Chappellaz, J., Davis, M., Delaygue, G., Delmotte, M., Kotlyakov, V. M., Legrand, M., Lipenkov, V. Y., Lorius, C., Pepin, L., Ritz, C., Saltzman, E., and Stievenard, M.: Climate and atmospheric history of the past 420,000 years from the Vostok ice core, Antarctica, Nature, 399, 429–436, 1999.
Petoukhov, V., Ganopolski, A., Brovkin, V., Claussen, M., Eliseev, A., Kubatzki, C., and Rahmstorf, S.: CLIMBER-2: A climate system model of intermediate complexity. Part I: Model description and performance for present climate, Clim. Dynam., 16, 1–17, 2000.
Pollard, D.: A coupled climate-ice sheet model applied to the Quaternary ice ages, J Geophys Res., 88, 7705–7718, 1983.
Ridgwell, A. J., Watson, A. J., and Raymo, M. E.: Is the spectral signature of the 100 kyr glacial cycle consistent with a Milankovitch origin?, Paleoceanography, 14, 437–440, 1999.

Ruddiman, W. F., Raymo, M. E., Martinson, D. G., Clement, B. M., and Backman, J.: Pleistocene evolution: Northern hemisphere ice sheets and North Atlantic Ocean, Paleoceanography, 4, 353–412, 1989.
Saltzman, B. and Maasch, K. A.: Carbon cycle instability as a cause of the late Pleistocene ice age oscillations: Modeling the asymmetric response, Global Biogeochem. Cycles, 2, 177–185, 1988.
Waelbroeck, C., Labeyrie, L., Michel, E., Duplessy, J. C., McManus, J. F., Lambeck, K., Balbon, E., and Labracherie, M.: Sea-level and deep water temperature changes derived from benthonic foraminifera isotopic records, Quat. Sci. Rev., 21, 295–305, 2002.
Zachos, J. C., Flower B. P., and Paul, H.: Orbitally paced climate oscillations across the Oligocene/Miocene boundary, Nature, 388, 567–570, 1997.

CPD
7, 2391–2411, 2011

Orbital forcing, carbon dioxide and regolith

A. Ganopolski and R. Calov

Table 1. List of model experiments.

Acronym	CO_2 concentration (ppm)	Orbital forcing	Initial time (kyr BP)	Sediment mask
BE (Baseline)	realistic	realistic	860	realistic
CCn	constant, $n = 180$ to 300, step = 20	realistic	860	realistic
CC$n/m$	constant, $n = 220$	realistic	$m = 800$ to 900, step = 20	realistic
CECn/e	constant, $n = 180$ to 300, step = 20	constant eccentricity, $e = 0.01$, 0.02, 0.03, 0.04, 0.05	860	realistic
COBn	constant, $n = 180$ to 300, step = 20	constant obliquity = 23.1°	860	realistic
REGn	constant, $n = 180$ to 300, step = 20	realistic	860	all continents covered by thick regolith

CPD
7, 2391–2411, 2011

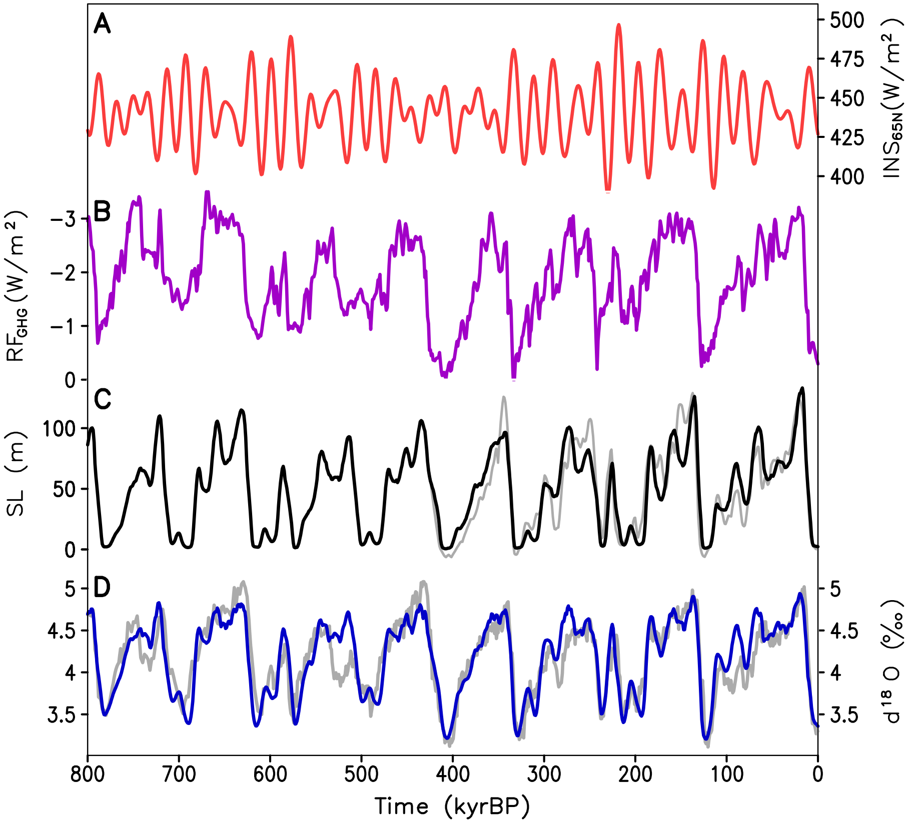

Fig. 1. (a) Maximum summer insolation at 65° N; **(b)** radiative forcing of prescribed equivalent CO_2 concentration; **(c)** simulated (black) versus reconstructed (grey) global ice volume (Waelbroeck et al., 2002); **(d)** simulated (black) versus reconstructed (grey) benthic $\delta^{18}O_c$ stack (Lisiecki and Raymo, 2005).

CPD
7, 2391–2411, 2011

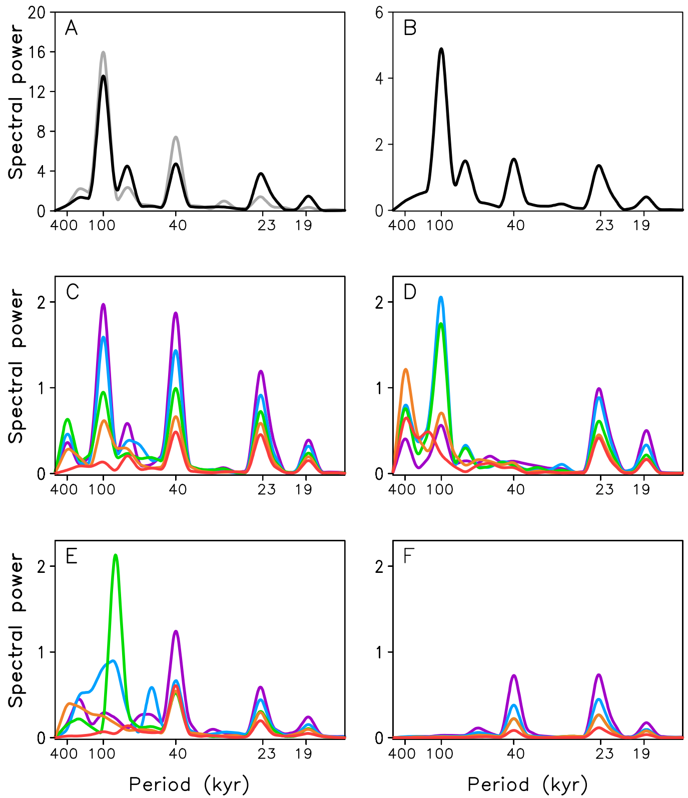

Fig. 2. **(a)** frequency spectrum of the simulated (black) versus reconstructed (grey) benthic $\delta^{18}O_c$ stack (Lisiecki and Raymo, 2005); **(b)–(f)** frequency spectra of the simulated ice volume: **(b)** baseline experiment, **(c)** CC*n* experiments with constant CO_2, **(d)** COB*n* experiments with constant obliquity, **(e)** CEC*n*/0.02 experiments with constant (0.02) eccentricity, **(f)** REG*n* experiments with continents completely covered by sediments. In **(c)–(f)**, purple lines correspond to a CO_2 concentration of 200 ppm, blue – 220 ppm, green – 240 ppm, orange – 260 ppm and red – 280 ppm.

CPD
7, 2391–2411, 2011

A. Ganopolski and R. Calov

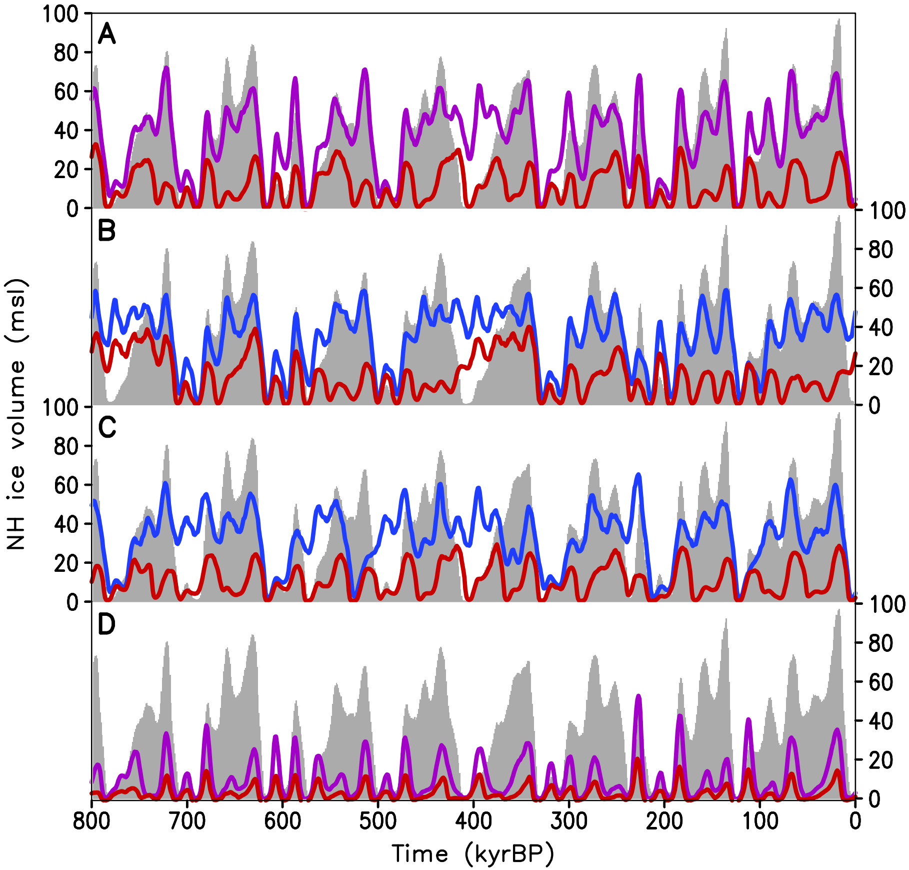

Fig. 3. Simulated ice volume variations in the subset of the experiments with constant CO_2 (colored lines) versus the Baseline experiment (grey shading). **(a)** CC*n* experiments, **(b)** COB*n* experiments (constant obliquity), **(c)** CEC*n*/0.02 experiments (constant eccentricity equal to 0.02), **(d)** REG*n* experiments (with continents completely covered by thick regolith layer). Purple lines correspond to a CO_2 concentration of 200 ppm, blue – 220 ppm and red – 280 ppm.

CPD
7, 2391–2411, 2011

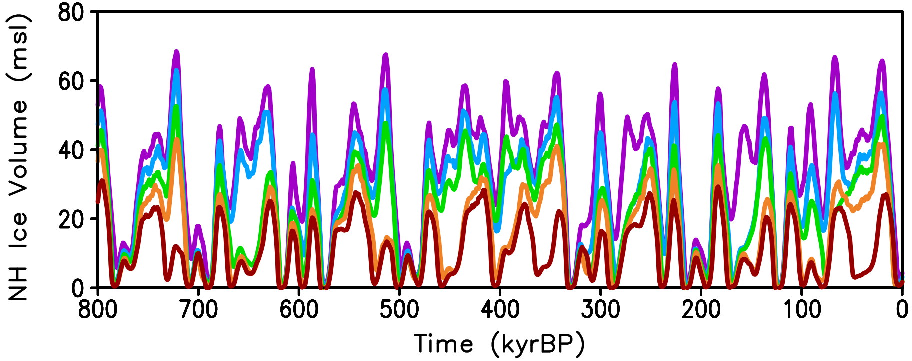

Fig. 4. Simulated ice volume variations in the experiments CC*n* (constant CO_2). The colours indicate the CO_2 levels: 200 ppm (purple), 220 ppm (blue), 240 ppm (green), 260 ppm (orange), 280 ppm (red).

CPD
7, 2391–2411, 2011

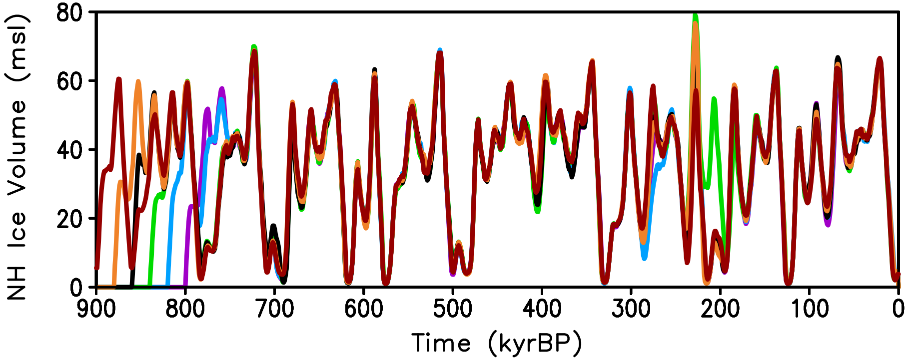

Fig. 5. Simulated ice volume variations in the experiments CC220/m starting from identical (interglacial) initial conditions but at a different time: $m = 900$ kyr BP (red), $m = 880$ kyr BP (orange), $m = 860$ (black), $m = 840$ (green), $m = 820$ (light blue) and $m = 800$ (blue) kyr BP.

CPD
7, 2391–2411, 2011

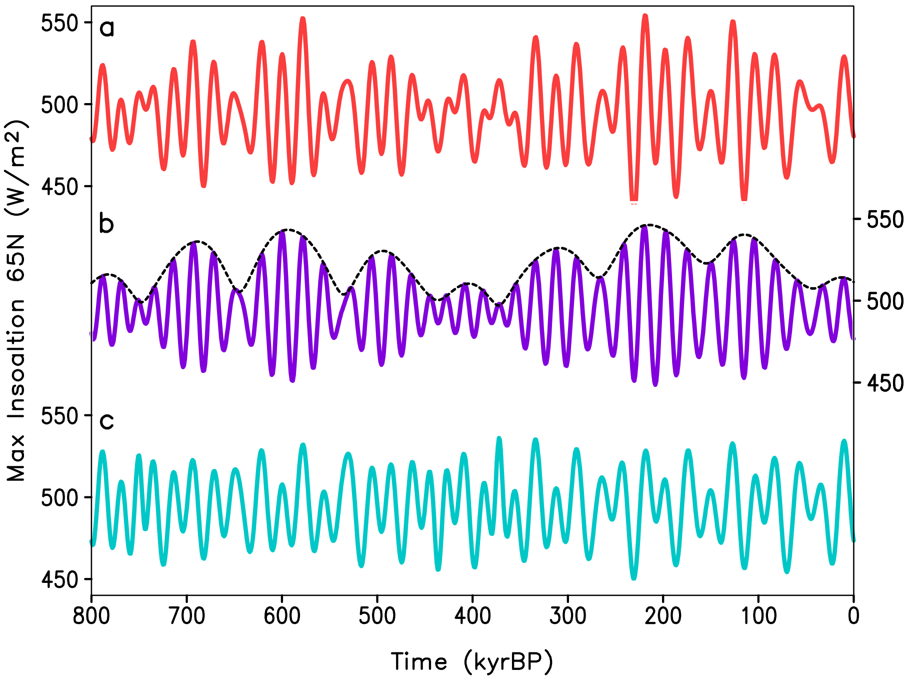

Fig. 6. Maximum summer insolation at 65° N in **(a)** the BE, CC*n* and REG*n* experiments, **(b)** the experiment with constant obliquity (COB*n*) and **(c)** constant eccentricity ($e = 0.002$, CEC*n*/0.02). The dashed line in panel **(b)** shows the amplitude modulation of the precessional cycle by eccentricity.

CPD
7, 2391–2411, 2011